Observations of Potential Gaia Red Dwarf Binaries in the Solar Neighborhood—III

Sophia Risin[1], Ivan Altunin[2], Rick Wasson[3], Russell Genet[4], and Simon Dye[5]

1. Stanford Online High School, sbrisin@ohs.stanford.edu
2. University of California, Berkeley, ialtunin@berkeley.edu
3. Orange County Astronomers, Murrieta, California, ricksshobs@verizon.net
4. California Polytechnic State University, San Luis Obispo, rgenet@calpoly.edu
5. University of Nottingham, Simon.Dye@nottingham.ac.uk

Abstract

Speckle interferometry observations were made of double stars within 30 parsecs of Earth with a late K or M dwarf component utilizing the Sloan r', i', and z' filters on the 11-inch telescope at the Fairborn Institute Robotic Observatory. Targets were selected with few or no prior observations except from Gaia. Data were reduced utilizing bispectrum phase reconstruction. Eleven red dwarf systems were observed, with two being reported as new discoveries. New astrometric measurements were extracted from UKIRT survey images.

1. Introduction

This project (hereinafter RDSN-III) is a continuation of the Red Dwarf (RD) Binaries in the Solar Neighborhood campaign initially started in 2019 with RDSN-I (Wasson et al., 2020), utilizing the Orange County Astronomers 22-inch telescope. It was continued in 2020 with RDSN-II (Altunin et al., 2020), also aimed at obtaining speckle interferometry measurements of binary stars that contain a red dwarf that are within the solar neighborhood. RDSN-II used the Fairborn Institute Robotic Observatory (FIRO) 11-inch telescope. In a supplemental paper, the data from these two studies were then compared to the UKIRT results with the somewhat surprising result that while our relatively bright targets were usually overexposed, the UKIRT astrometric measurements were of comparable quality to the OCA and FIRO speckle observations, both agreeing well with Gaia astrometry (Altunin et al., 2021).

This current paper, RDSN III, continues the series of RD speckle observations, placing greater emphasis on binaries thought to have short periods. This was motivated by the potential of seeing significant orbital motion using historical data from GAIA and UKIRT which, in combination with our data points, spanned a decade of time. New astrometric measurements were extracted from UKIRT survey images in the same way as described in Altunin et al., 2021.

2. Target Selection

Information on potential targets was obtained using the Gaia Double Star Selection tool (Rowe, 2018) to access his Gaia DR2 Double Star (GDS) catalogue. An example of the GDS input and output data is shown in Figure 1. Candidates for this project were selected to be observable by FIRO in the fall evenings, lie within 30 parsecs from the Sun, and have relatively short periods roughly estimated from Gaia DR2 data alone, as described below.

Distance (parsecs) = 1000 / Parallax (mas)

Note: Distance to the primary is best to use as it should have the lowest error being the brightest.

*Lateral Physical Separation (AU) = Distance (parsecs) * Apparent Lateral Separation (arc seconds)*
Absolute Magnitude = Apparent Magnitude (Gaia G Mag) – 5[Log Distance(parsecs) – 1]
Luminosity = Absolute Magnitude

Note: We dispensed with bolometric correction

Luminosity Star / Luminosity Sun = 2.512 ^ (4.83 – Luminosity Star) Note: 4.83 is solar luminosity
Mass (solar units) = Luminosity (solar units) ^ 0.25

Note: "valid" for 0.033 < Luminosity (solar units) < 16 (Solaris et al., 2005)

Period (years) = SQRT {[Lateral Separation (AU)]^3 / [Mass Primary + Mass Secondary (solar units)]}

Note: This assumes a circular orbit, perpendicular to the line of site, okay for our rank-ordering purposes. Highly elongated orbits with separations observed near perihelion will give period estimates wide of the mark, albeit not orders of magnitude off.

We originally thought that we would need some sort of prefilter to toss out optical binaries and systems with missing secondary data, bad Gaia data, etc., but, somewhat surprisingly, the period algorithms seem to get rid of almost all of these problems.

In addition, targets were selected to have either no entry or few reported observations in the Washington Double Star (WDS) catalog. Only WDS targets with less than 40 past observations were retained. This yielded 11 of the targets, two of which were not listed in the WDS. All these stars have similar Gaia parallax and proper motion, so they are likely to be gravitationally bound binaries or at least common proper motion pairs.

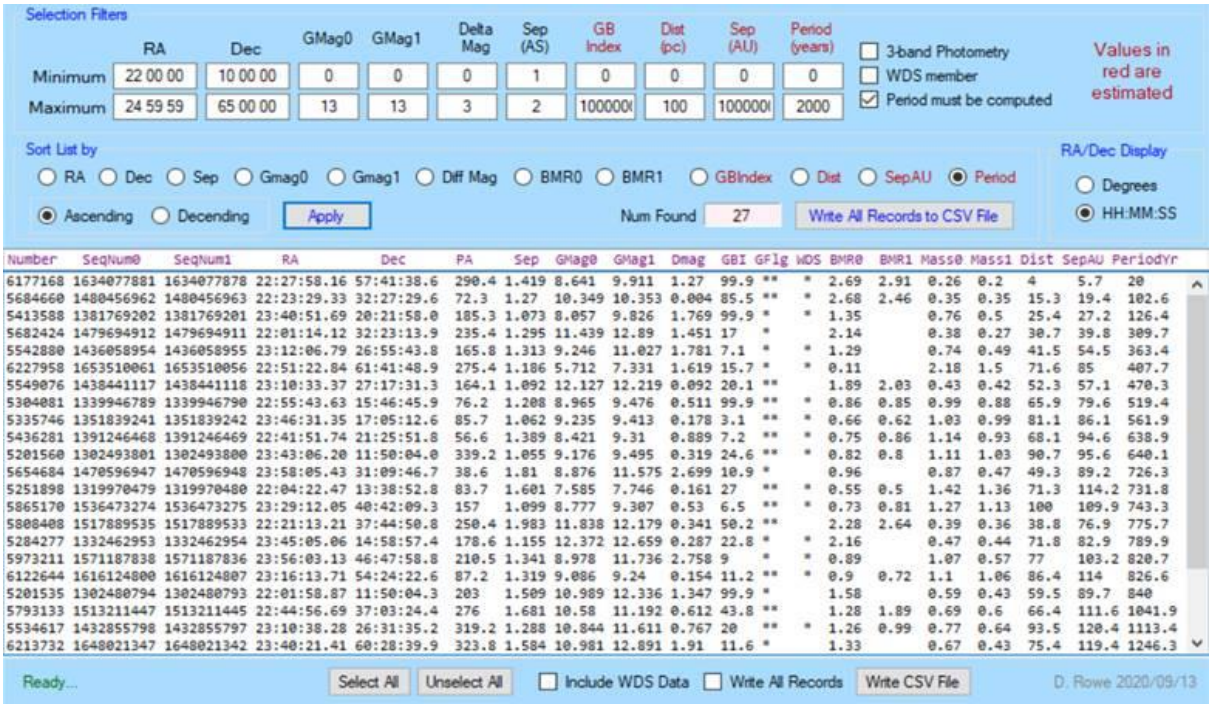

Figure 1: Gaia Double Star Selection tool. Selection filters include the specific parameters for the targets generated.

Table 1: Gaia Information. Column 1, J2000 coordinates. Column 2, Gaia primary/secondary mags. Remaining columns are the Bp-Rp for primary/secondary, approximate spectral type taken from its plotting on the HR Diagram from RD I, the proper motion in RA for the primary/secondary (mas), the proper motion in Dec for the primary/secondary (mas), the parallax for the primary/secondary (mas), and the WDS name if known.

Coords (2000) UCAC4	$GMag_A$ $GMag_B$	$(Bp - Rp)_A$ $(Bp - Rp)_B$	Spec	$PMRA_A$ $PMRA_B$	PMD_A PMD_B	π_A π_B	WDS Discovery
222329.09+322733.5	10.349 10.353	2.682 2.465	M M	254.849 244.4067	-170.2115 -251.6855	65.48 65.86	WOR 11
003317.5+341910	13.304 13.43	2.999 3.012	M M	100.4 82.7	-56.9 -59.5	40.63 40.54	N/A
225740.94+371923.6	11.843 13.782	2.553 3.02	M M	-548 -566.2	-364.9 -355.3	43.03 41.9	KPP3388
235526.8+221133	8.435 12.203	1.23 1.888	F/G K	202 194.9	-146.9 -111.8	39.18 34.8	N/A
031614.02+581001.4	10.011 10.186	2.25 2.3	K/M K/M	444.4 415.1	-324.5 -318.3	73.76 73.74	MLB 115AB
000541.03+454843.3	8.248 6.191	1.856 1.88	K K	888.6 845.9	-162.5 -148.5	86.87 86.94	STT 547AB
015428.04+574127.9	11.458 13.568	2.691 2.874	M M	-25 -31.6	-197.2 -205.8	44.93 44.64	NSN1
041310.12+503141.3	12.7 13.254	2.849 2.724	M M	-395.7916 -394.3805	-194.8368 -176.1289	50.18 50.49	CHR 15
032406.48+234706.1	9.948 10.789	2.066 2.088	K K	215.0504 200.9	-120.2 -114.3	48.3 48.09	WOR 4AB
035428.03+163657.8	6.638 10.408	0.894 1.995	F/G K	214.2 209.9	-167.3 -194.5	48.81 48.92	HEI 31
015912.38+033109.3	10.455 11.134	2.017 2.536	K M	263.1 266.2	24.1 43.5	41.77 41.72	LDS3331

3. Instrumentation and Procedures

The FIRO telescope is an 11-inch Celestron C-11 Schmidt Cassegrain telescope (Figure 2) with an f/10 focal ratio and nominal 1.5 X Barlow with an effective focal length of 4200 mm. It is controlled by the Sidereal Technology Servo Controller on a custom equatorial “L” mount (Altunin et al., 2020).

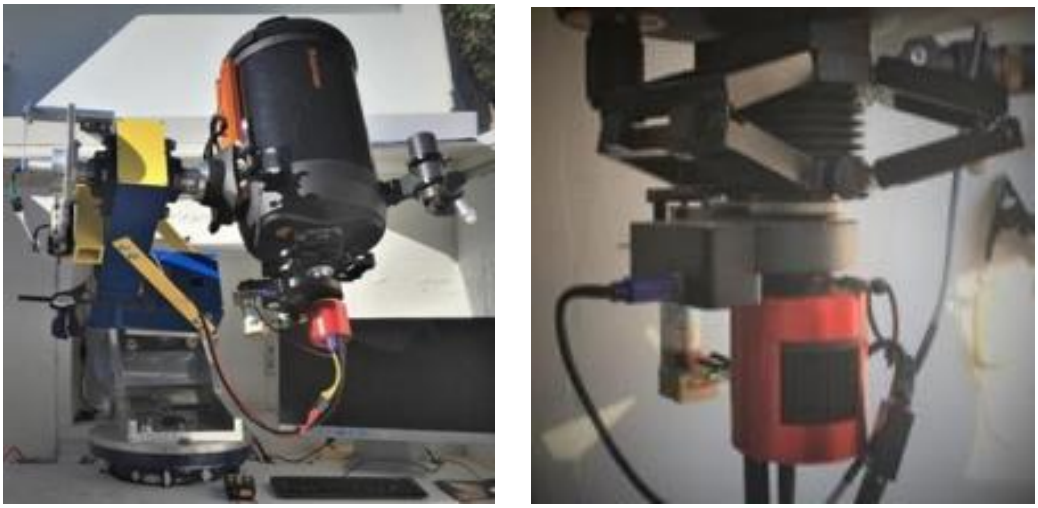

Figure 2. *Left: The "L" mount sitting on top of an equatorial wedge which supports the Celestron C-11 optics. Right: the instrument cluster includes a Clement focuser, a ZWO filter wheel, a 1.5 X Barlow, and CMOS camera.*

The instrument payload consists of a focuser, filter wheel, Barlow and CMOS camera. The five-position ZWO motorized filter wheel contains a clear "filter," and four Sloan filters: g′ r′, i′, and z′ although the g′ and clear filters were not used in this research. The CMOS camera is a thermoelectrically-cooled (40-50°C below ambient) ZWO ASI 1600 MM, selected for its low read noise (only 1.2e), small pixel size (3.8 microns), and relatively large format (16 megapixels, 4636x3520).

In observing RDs with the 11-inch FIRO telescope, many short integrations ranging in time from 0.01 to 2.0 seconds were utilized to perform speckle and quasi-speckle interferometry. Speckle interferometry, it might be noted, is a process of using short exposures and Fourier transforms to resolve close double stars. Some of the stars in this paper were bright enough for classical short speckle exposures, but others required longer ("quasi-speckle") exposures, as explored in depth in RD-II (Altunin et al., 2020). Bispectrum (triple correlation) processing corrects the distorted wavefront phase to produce a reconstructed, diffraction-limited image. An example Bispectrum image is shown in Figure 3.

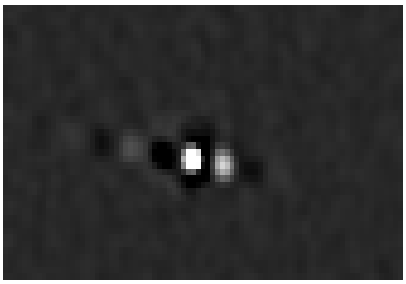

Figure 3. *An example of a reconstructed image* ***of*** *WOR11 in the r' filter. Orientation is North up, East left.*

To reduce the data, Speckle Toolbox 1.14 (Rowe 2020) was used. The data reduction started with calibration of the plate scale and camera orientation from plate-solved, full-frame images taken each night. Speckle images were taken in the region of interest (ROI) mode. These images were made into FITS cubes, with one cube made per filter. Following the creation of FITS cubes, bispectrum (triple correlation) phase reconstruction was conducted. After phase reconstruction, the position angle and separation were measured.

4. Results

The targets were observed November 12 to December 18, 2020, ~5.4 years after the Gaia epoch 2015.5 observations. Several systems were observed multiple times on the same night to improve precision. Astrometry results are summarized in Table 2.

Table 2: Speckle Astrometric Results. Column 1 is the Besselian observation date. Column 2 is target RA and Dec Coordinates (2000.0) in hhmmss.s+ddmmss format. The remaining columns are the average Position Angle (θ) in degrees, standard deviation of Position Angle, Standard Error of Position Angle, average Separation (ρ), standard deviation of Separation, and the standard error of separation in arc-sec. The Average, Standard Deviation and Standard Error results include all filters and multiple-night data, weighted equally regardless of quality.

Date	Coord (2000)	θ	Std Dev	Std Error	ρ	Std Dev	Std Error
2020.865	222329.09+322733.5	251.56	1.62	1.62	1.185	0.039	0.014
2020.871	003317.5+341910	174.05	2.18	1.26	3.161	0.086	0.050
2020.871	225740.94+371923.6	214.87	N/A	N/A	2.669	N/A	N/A
2020.871	235526.8+221133	290.08	0.28	0.19	2.589	0.047	0.033
2020.912	031614.02+581001.4	359.82	0.20	0.14	5.061	0.025	0.018
2020.912	000541.03+454843.3	187.59	0.42	0.16	5.990	0.013	0.005
2020.942	015428.04+574127.9	3.59	N/A	N/A	8.595	N/A	N/A
2020.961	041310.12+503141.3	38.94	0.67	0.38	1.890	0.038	0.022
2020.961	032406.48+234706.1	329.26	0.81	0.33	2.622	0.028	0.012
2020.964	035428.03+163657.8	236.84	0.13	0.05	3.548	0.176	0.072
2020.967	015912.38+033109.3	52.27	N/A	N/A	3.874	N/A	N/A

Historical data from UKIRT was reduced by one of us (SD) for 6 of the 11 targets, using the procedures outlined in Altunin et al., 2021. The results are shown in Table 3. The remaining 5 stars were unable to be resolved or no UKIRT data existed.

Table 3: Column 1 is the target RA and Dec Coordinates (2000.0) in hhmmss.s+ddmmss format. The remaining columns are the Gaia 2015.5 position Angle and Separation measurements, the Besselian date of UKIRT observations, and UKIRT position Angle and Separation measurements. Cells with UKIRT data omitted were unable to be resolved.

Coord	Gaia θ	Gaia ρ	UKIRT date	UKIRT θ	UKIRT ρ
222329.09+322733.5	72.27	1.270			
003317.5+341910	174.64	3.147	2013.9277	174.95	3.05
225740.94+371923.6	210.49	2.522	2013.7367	204.22	2.41
235526.8+221133	286.68	2.370			
031614.02+581001.4	2.12	5.039	2012.8435	1.28	4.94
000541.03+454843.3	188.21	6.038	2014.9414	183.77	6.24
015428.04+574127.9	0.46	8.673	2016.7867	0.79	8.65
041310.12+503141.3	51.33	1.637			
032406.48+234706.1	339.85	2.588			
035428.03+163657.8	239.17	3.554			
015912.38+033109.3	54.3	4.170	2011.5867	54.83	4.08

5. Analysis

Seven observed systems in Table 2 showed statistically significant movement since the Gaia DR2 2015.5 reported positions, with six of them being present in the WDS and having discovery codes. Historical measurements of all the systems are plotted and further analyzed below with our data (red triangle) and WDS and Gaia data in Figure 4.

The historical data of WDS 22234+3228 WOR11 are plotted in Figure 4 with our measurement indicated by the red triangle. As shown, our data measurement is consistent with the other historical data and falls along a potential curve indicating orbital motion. The Gaia position angle θ = 72.27 (Table 3) is approximately 180 degrees different from our observation (Table 2 and Figure 3). The likely cause is that the two stars are extremely close in Gaia G magnitude (10.349 and 10.353, Table 1). Their ΔG magnitude is only 0.0040, almost within the Gaia DR2 combined uncertainty ΔG=0.0029. Therefore, the primary and secondary identities are apparently reversed in the broad G band, resulting in a 180-degree difference in θ. This is substantiated by Gaia DR2 color measurements; although slightly brighter in G, Gaia's "primary" is actually a redder, cooler star than its "secondary" - ("primary" color index Bp-Rp=2.682, Teff=3693K; "secondary" Bp-Rp=2.465, Teff=3820K). Therefore, 180 degrees has been added to the Gaia position angle in Figure 4, where all the measurements are in good agreement.

Our measurements as plotted in Figure 4 correspond to the systems of WDS 00057+4549 STT 547AB and 03162+5810 MLB115AB, and are plotted with the historical WDS data. MLB 115AB has the potential for future papers calculating its period from the new data. STT 547AB had the presence of scattering in the observations. Both systems are consistent with these orbital solutions, following the same trend as historical data points and lying on the proposed orbit. The graph of WDS 03243+2347 WOR 4AB in Figure 4 has our observation about a ½ arcsecond off the proposed orbital solution and so further observations are warranted.

Future observations are needed for NSN 1 and CHR 15 to determine period and curvature. For WOR 4AB, the observation had a high amount of error but has the potential to be the turning point in the orbit. Future observations are required to determine if this is the case. Future observations are needed to determine the orbital behavior of HEI 31. LDS3331 appears to have a near linear path and future observations are needed to determine its behavior.

The system 003317.5+341910 was found in WDSS, with only 2MASS and Gaia prior observations, but is not present in the WDS nor has a discovery designation. Therefore, it is reported as a new system but did not show statistically significant motion since Gaia. The system 235526.8+221133 was not found in the WDSS and has only Gaia as a prior observation. It is reported as a new system and shows statistically significant motion. For 235526.8+221133, UKIRT was overexposed and unable to be reduced. Future observations are warranted to determine presence of curvature. The parallax values for these systems are shown in Table 1.

Three of the reported measurements are consistent with existing preliminary orbit solutions and are also reported here. Our analysis shows that 7 of the observed systems showed statistically significant motion.

Figure 4: Orbits. Plots include positions of each star (Dec, RA) including the measurements from the WDS as well as current (red triangle), UKRIT is denoted with the orange triangle. Other coloring is by the scale on the right of the graph with more blue colors being more recent observations from the Washington Double Star Catalog.

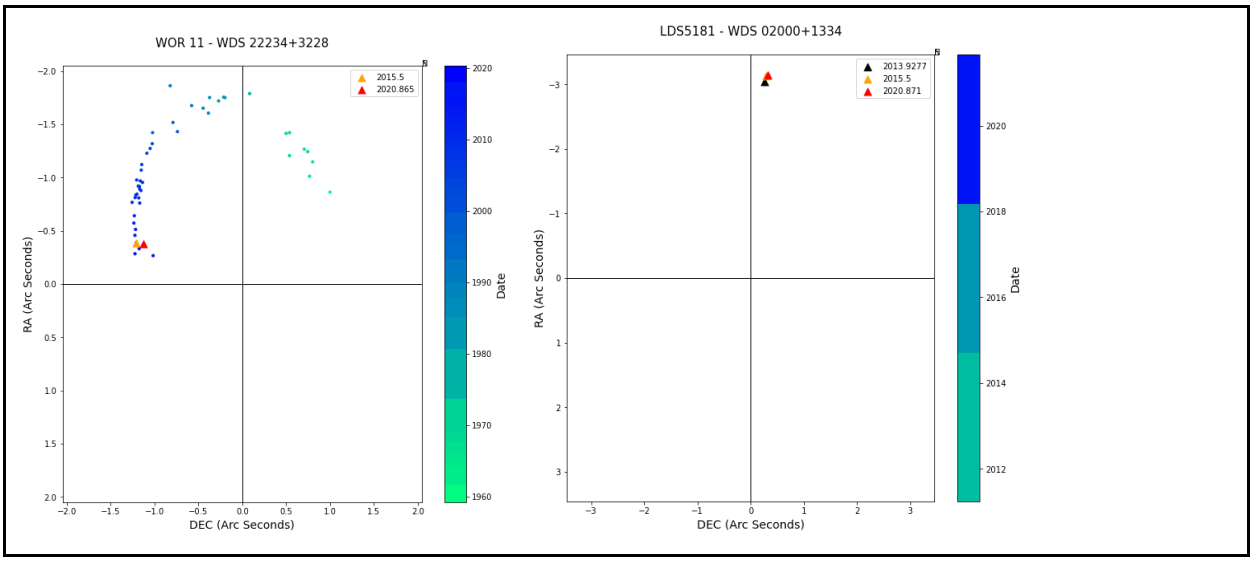

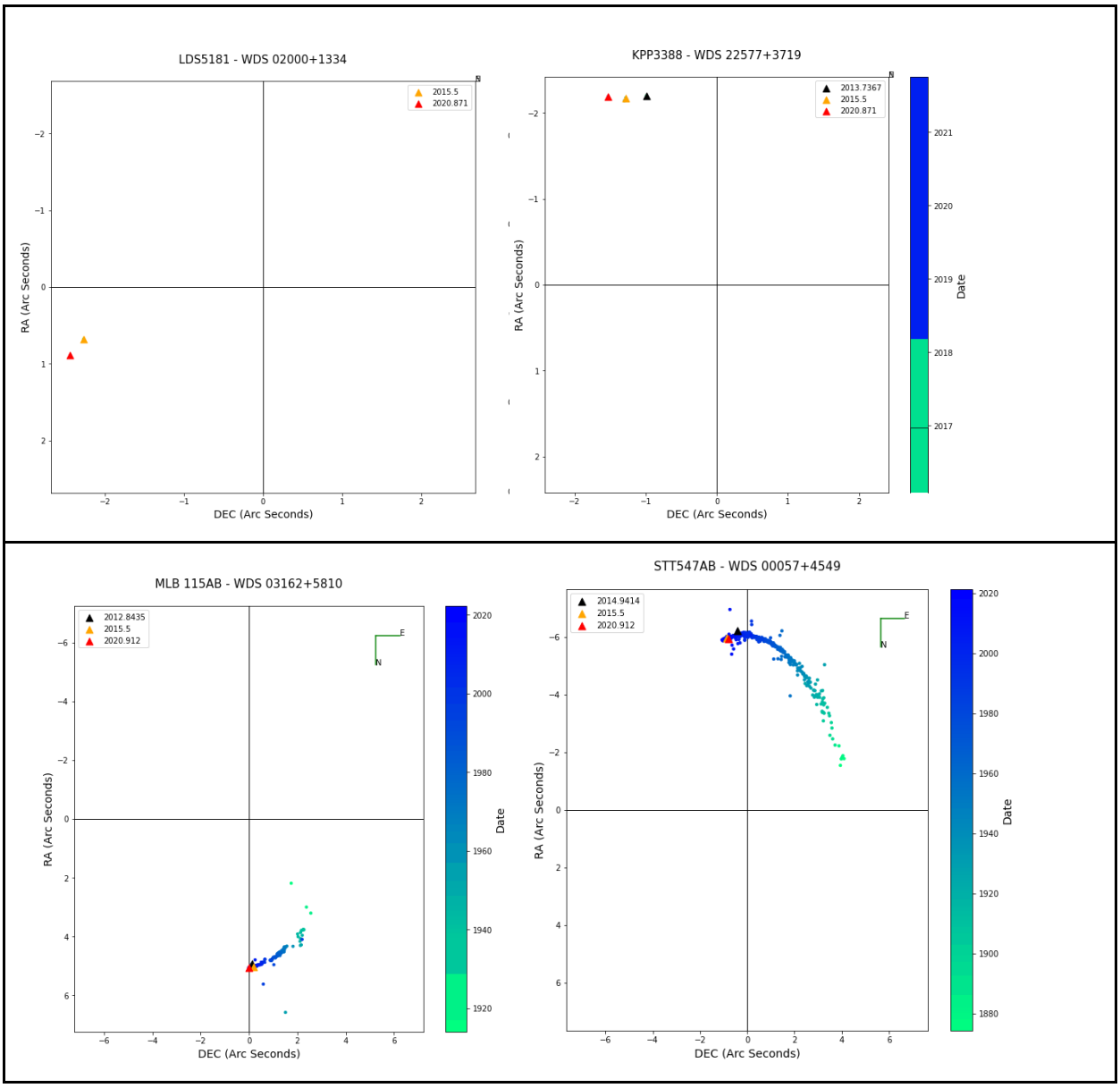
LDS5181 - WDS 02000+1334
2015.5
2020.871
RA (Arc Seconds)
DEC (Arc Seconds)
KPP3388 - WDS 22577+3719
2013.7367
2015.5
2020.871
Date
MLB 115AB - WDS 03162+5810
2012.8435
2015.5
2020.912
STT547AB - WDS 00057+4549
2014.9414
2015.5
2020.912
E
N

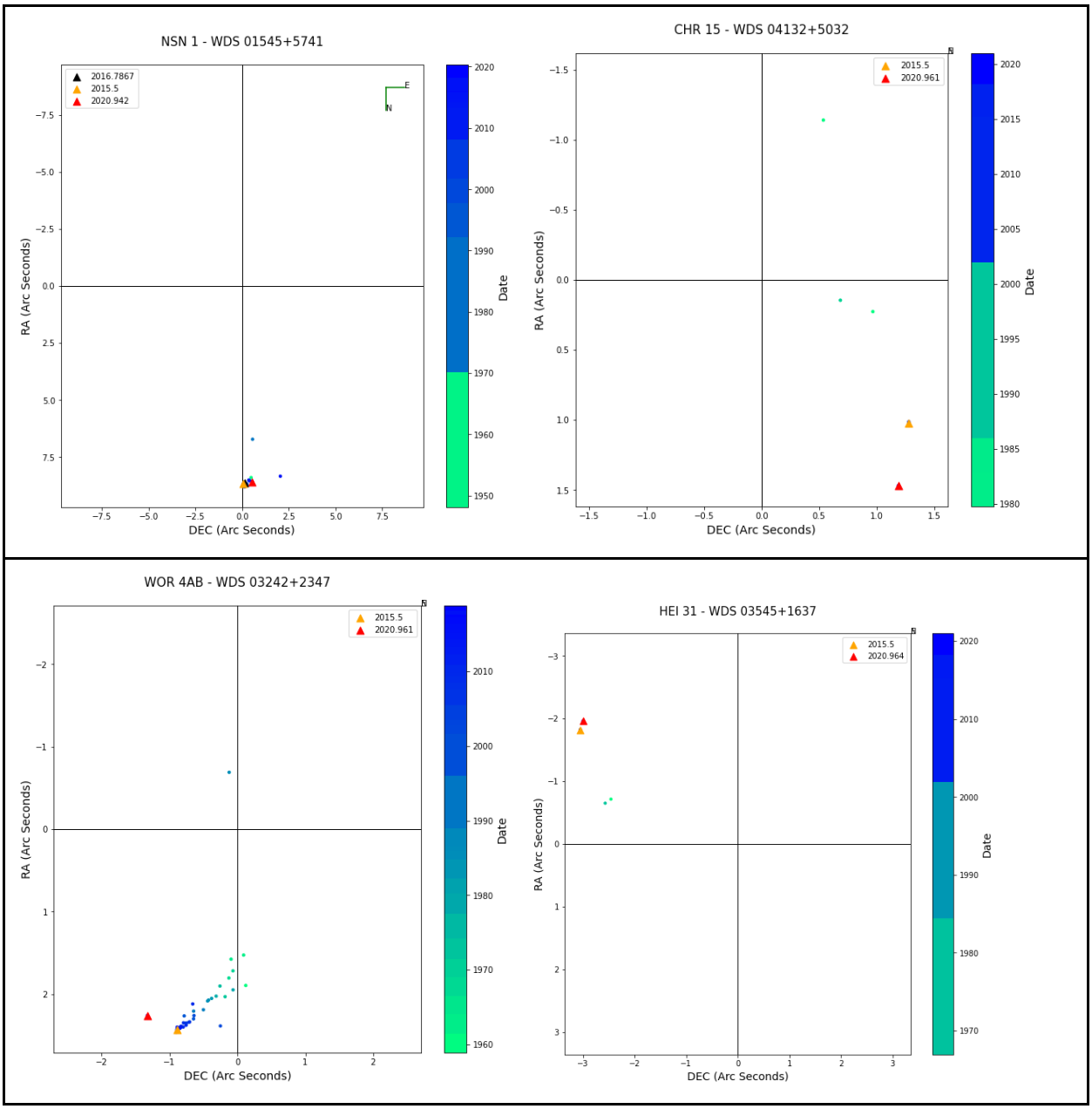
NSN 1 - WDS 01545+5741
2016.7867
2015.5
2020.942
E
N
RA (Arc Seconds)
DEC (Arc Seconds)
Date
CHR 15 - WDS 04132+5032
2015.5
2020.961
RA (Arc Seconds)
DEC (Arc Seconds)
Date
WOR 4AB - WDS 03242+2347
2015.5
2020.961
RA (Arc Seconds)
DEC (Arc Seconds)
Date
HEI 31 - WDS 03545+1637
2015.5
2020.964
RA (Arc Seconds)
DEC (Arc Seconds)
Date

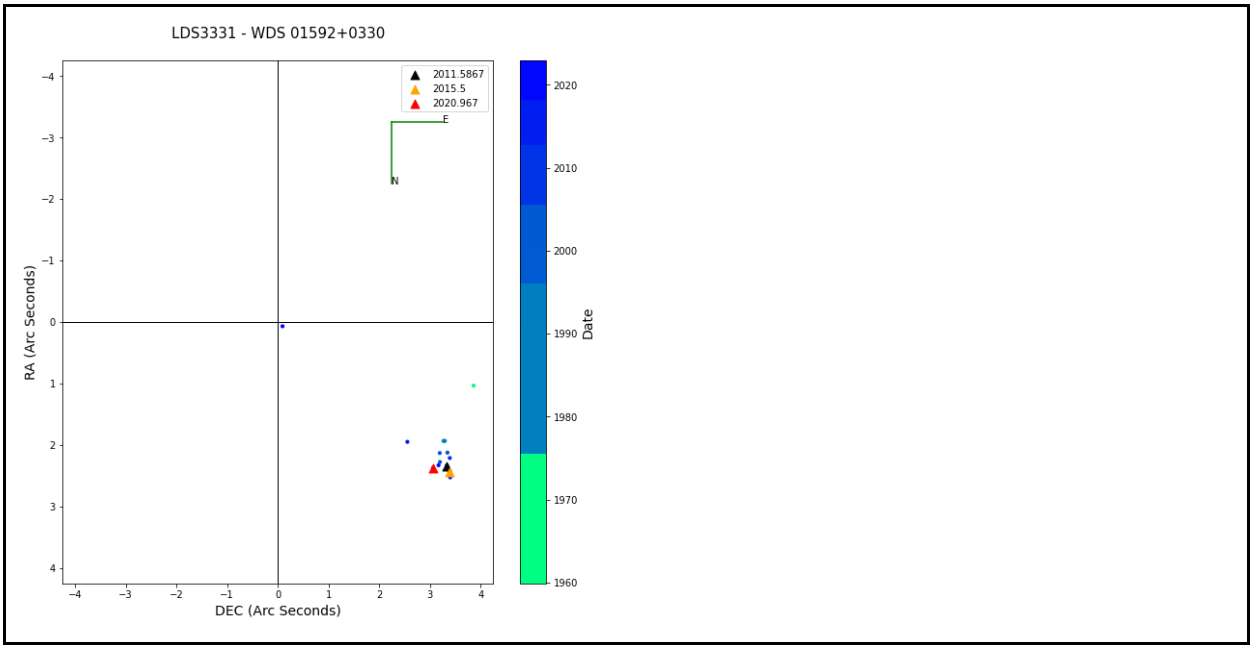

The new binary systems are shown in Table 4 below with their Gaia measurements and current measurements. 235526.8+221133 shows motion in position angle greater than the error. 003317.5+341910 shows motion but within the estimates for error.

Table 4: Potential New Binaries. Column 1 includes the coordinates of the system. The remaining columns contain the Gaia position angle, Gaia separation, our position angle, the standard error of the position angle, our separation, the standard error of our separation, the delta position angle, and delta separation.

Coords	Gaia θ	Gaia ρ	θ	θ error	ρ	r error	Delta θ	Delta ρ
235526.8+221133	286.68	2.370	290.08	0.19	2.589	0.033	3.40	0.219
003317.5+341910	174.64	3.147	174.05	1.26	3.161	0.050	0.59	0.014

6. Conclusions

This paper built on the prior research conducted in RD-I and RD-II by examining potential binaries with smaller separations as well as incorporating additional data from UKIRT. Eleven binary systems containing either a red dwarf companion or both being red dwarfs were observed. Most systems demonstrated significant motion since Gaia DR2. This project continued the observations of red dwarf binaries carried out with the Orange County Astronomers 22-inch telescope and observed in multiple Sloan Bands (r' i' z'). Faster moving stars with shorter periods were observed and statistically significant motion was detected. Our techniques for conducting remote real time speckle interferometry were improved. UKIRT data were obtained to add to the historical record, and extend astrometric coverage
of new and under-observed systems for nearly a decade.

Acknowledgements

We acknowledge David Rowe's development of the Gaia Double Star (GDS) database and tool and the Speckle ToolBox (STB), both critical to the success of this project. RG thanks Rowe for contributing the ZWO ASI 1600 camera to the Fairborn Institute Robotic Observatory, Kevin Iott for contributing the PlaneWave Instruments worm-drive assemblies, and Dan Gray for contributing the Sidereal Technology control system. We also thank Dan Gray for providing the Sidereal Technology SiTech ZWOCam software for the project and his responsiveness to requests for making software improvements. Finally, we thank the European Space Agency and the Gaia team for the use of their observations, and the U.S. Naval Observatory for the use of the Washington Double Star Catalog and 6th Orbit Catalog. This work has made use of data from the European Space Agency (ESA) mission Gaia, processed by the Gaia Data Processing and Analysis Consortium. Funding for the DPAC has been provided by national institutions, in particular the institutions participating in the Gaia Multilateral Agreement.

References

Altunin, I., Wasson, R., & Genet, R., 2020. "Observation of Gaia (DR2) Red and White Dwarf Binary Stars in the Solar Neighborhood - II," Journal of Double Star Observations, 16-5, 470.

Altunin, I., Risin, S., Genet, R., Dye, S., Wasson, R., & Rowe, D, 2021. "Comparison of Recent Small Telescope Speckle Interferometry with Gaia and Archived 3.8-Meter UKIRT J-Band Image Astrometry," Journal of Double Star Observations, 17-2, 104.

Marchetti, C., Caputo, R., & Genet, R., 2020. "The Fairborn Institute Robotic Observatory: First Observations," submitted to the Journal of Double Star Observations

Salaris, Maurizio; Santi Cassisi (2005). *Evolution of stars and stellar populations*. John Wiley & Sons. pp. 138–140. ISBN 978-0-470-09220-0.

Wasson, R., Rowe, D., & Genet, R., 2020. "Observation of Gaia (DR2) Red and White Dwarf Binary Stars in the Solar Neighborhood," Journal of Double Star Observations, 16-3, 208.

Rowe, D., 2018, "GDS1.0 Gaia (DR2) Double Stars Search Program." Private communication

Rowe, D., & Genet, R., 2015. "User's Guide to PS3 Speckle Interferometry Reduction Program, Journal of Double Star observations, 11, 266.